



TCNE and TCNQ ligands as efficient bridges in mixed-valence complexes containing iron–cyclopentadienyl and other organometallic systems

Carlos Diaz^{a,*}, Alejandra Arancibia^b

^aDepartamento de Química, Facultad de Ciencias, Universidad de Chile, Casilla 653, Santiago, Chile

^bFacultad de Química, P. Universidad Católica de Chile, Casilla 306, Santiago, Chile

Received 10 May 1999; accepted 4 October 1999

Abstract

Reaction between the π -accepting tetracyanoethene (TCNE) or tetracyano-*p*-quinodimethane (TCNQ) ligands and the π -electron-rich organometallic species $\text{Cp}(\text{dppe})\text{Fe}^+$ results in the formation of the complexes $[\{\text{Cp}(\text{dppe})\text{Fe}\}_n\{\eta^n\text{-TCNX}\}](\text{PF}_6)_n$ ($n = 1, 2$ and 4). Infrared spectroscopy, magnetic moment measurements, electron-spin resonance (ESR) and cyclic voltammetry data indicate a net transfer of one π electron to the TCNX acceptor ligand. The polynuclear complexes have an intense intervalence electron transfer absorption band in the near-infrared region. The values for the intervalence parameters $\alpha = 0.02\text{--}0.06$ and $V_{\text{ab}} = 200\text{--}600\text{ cm}^{-1}$ indicate that these complexes can be classified as class II according to Robin-Day. Estimation of the rate of electron transfer affords values in the order of 10^8 s^{-1} , which are compared and discussed with values estimated for other polynuclear systems containing TCNE and TCNQ ligands as bridges. The solvent effect on the intervalence transition follows Hush's prediction for highly polar solvents, thereby permitting evaluation of the reorganizational energy. For the related series $[\{\text{Cp}(\text{dppe})\text{Fe}\}_n(\mu\text{-X})](\text{PF}_6)_n$, the reorganization energy appears to depend mainly on the inner reorganization energy through changes to vibrational modes of the bridge. Reorganizational energy is not as important in determining the electron transfer rate as the activation energy, E_a . A linear relationship is found between the rate constant $\ln(k_{\text{et}})$ and the activation energy. These results can be discussed within the Marcus theory of electron transfer. The fast and efficient electron transfer between the metal fragments is discussed using molecular orbital arguments. ©2000 Elsevier Science Ltd All rights reserved.

Keywords: Hush theory; Iron complexes; Mixed valence; TCNE complexes; TCNQ complexes

1. Introduction

Tetracyanoethene (TCNE) and the related tetracyano-*p*-quinodimethane (TCNQ) are molecules that present interesting acceptor properties, which are associated with their unusual electrical and magnetic behaviour [1–4]. TCNE and TCNQ can act as σ ligands (via the nitrile-N lone pair) as a π -type arrangement (via the C=C olefinic bond in TCNE) or 'free' (ion pair) mode II (Fig. 1) [5].

Many coordination compounds with considerable metal ligand delocalization have been reported [6–10]. Several special features make such compounds interesting for practical purposes: (1) intense charge-transfer absorption bands in the visible and near-infrared regions can make such systems useful as dyes for information storage using optic fibre and diode laser [11,12]; (2) the communication between metal-connected ligands and/or ligand-connected metals has

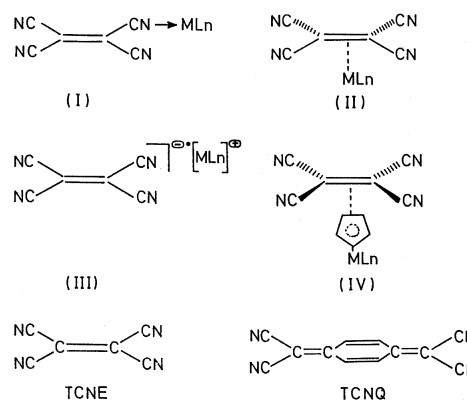


Fig. 1. Coordination modes of TCNE and TCNQ ligands.

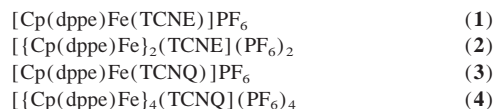
received attention in the area of low-dimensional polymers with electron-propagating capabilities and within the concept of 'molecular electronics' [13]; (3) the existence of several close-lying and easily accessible redox transitions renders

* Corresponding author. Tel./fax: +56-2-271-3888

these compounds suitable as ‘electron reservoirs’, especially because small structural changes during the redox transitions of extensively delocalized systems favour rapid electron transfer due to the small reorganization barriers [14–16].

Non-reduced TCNE and TCNQ are rather poor ligands for metal centres; however, on electron uptake by back-donation or full reduction with one or two electrons, they can bind metal fragments via modes I–IV.

In connection with points (2) and (3), we report here the preparation of the complexes [$\{\text{Cp}(\text{dppe})\text{Fe}\}_n\{\eta^n\text{-TCNX}\}(\text{PF}_6)_n$] and the study of the intermetallic electron transfer in the following polynuclear systems:



While several di- and polynuclear complexes with extensive π delocalization including the metal centre have been reported [6–10], no detailed quantitative studies on the electron transfer via TCNE and TCNQ bridges have been reported.

We have selected the fragment $\text{Cp}(\text{dppe})\text{Fe}^+$ because its electron richness permits efficient electronic delocalization [11–21], it binds strongly to nitrogen cyanide containing ligands [22–25] and the iron in the fragment is electrochemically active [11–21].

2. Results and discussion

2.1. Mononuclear complexes

$\text{Cp}(\text{dppe})\text{FeI}$ reacts with an excess of TCNE or TCNQ in the presence of NH_4PF_6 or TIPF_6 in CH_3OH or CH_2Cl_2 ,

respectively, to give dark black–green solids whose elemental analysis and spectroscopic properties agree with the mononuclear formulation $[\text{Cp}(\text{dppe})\text{Fe}(\text{TCNX})]\text{PF}_6$. As observed for another d^5 paramagnetic mononuclear complex $[(\text{C}_5\text{R}_5)\text{Mn}(\text{CO})_2(\eta^1\text{-TCNX})]$ and others [8–10], magnetic resonance investigations of complexes **1** and **3** have been hampered by the paramagnetism of the complexes. The dark-black colour is typical of complexes of the type $\text{Cp}(\text{dppe})\text{Fe}^{\text{III}}$ [19–21]. Additional evidence for the reduction of the TCNX ligand is provided by IR spectra [5] (see Table 1). As for other monodentate TCNX complexes, three ν_{CN} bands were observed [26] as expected for the non-symmetrically bound ligands [5,27–33]. The ν_{CN} IR bands are quite intense and shifted to lower wavenumbers compared to those of the free, non-reduced ligands. This indicates nitrile-N coordination and sizeable back-donation of π electron density from the metal fragments to the TCNX ligand [5,27–33]. The ν_{CN} wavenumber of the complexes lies between those of the free anion radicals and the values found for the dianions.

Thus, the mononuclear complexes are distinguished from polynuclear complexes and from the free ligands as the highest intensity is displayed by the low-energy band for the polynuclear systems [6–10]. In the IR spectra of complexes **1** and **3** the highest intensity corresponds to the high-energy band. IR bands for the $\text{Cp}(\text{dppe})\text{Fe}^+$ fragment appear normally [34]; the main values are displayed in Table 1.

2.1.1. Magnetic measurements

Magnetic moments for complexes **1** and **3** are typical values for $[\text{Cp}(\text{dppe})\text{FeX}]^+$ complexes [19,20], corresponding to one unpaired electron in low spin Fe^{III} . The unpaired electron arising from the radical TCNX^- could not be observed due to spin coupling between them in solid state.

Table 1
IR data for complexes 1–4^a

Complex	$\nu(\text{C}_5\text{H}_5)$ ^b	$\nu(\text{dppe})$ ^c	$\nu(\text{PF}_6)$	$\nu(\text{CN})$	
				Solid	Solution
TCNE				2257	2251
[$\text{Cp}(\text{dppe})\text{Fe}(\text{TCNE})]\text{PF}_6$ (1)	1098	696	843	2220	2210
				2171	2200
				2059	2136
				1995	2065
[$\{\text{Cp}(\text{dppe})\text{Fe}\}_2(\text{TCNE})](\text{PF}_6)_2$ (2)	1106	706	847	1994	1994
				2197(sh)	2197(sh)
				2173	2173
TCNQ				2223	2223
[$\text{Cp}(\text{dppe})\text{Fe}(\text{TCNQ})]\text{PF}_6$ (3)	1094	694	847	2173	2185
				2128	2129
				2067	
				2099	2114
[$\{\text{Cp}(\text{dppe})\text{Fe}\}_4(\text{TCNQ})](\text{PF}_6)_4$ (4)	1096	697	838	2032	2035

^a In KBr pellets, unless other indicated; data given in cm^{-1} .

^b $\delta(\text{C-H})$ bending in-plane vibration.

^c $\delta(\text{C-H})$ bending out-of-plane vibration.

Table 2
Long-wavelength absorption maxima λ (nm), magnetic and ESR data for TCNX complexes

Complex	λ_{\max}^a (CH ₂ Cl ₂)	μ (eff) ^c	ESR ^c : g_1, g_2, g_3
1	545 (1187), 619 (1245)	1.8	2.0189; 2.1912; 2400
2	441 ^b (2262), 512 (1769) ^b , 1073 (969)	0.7	1.9880; 2.2086; 2.420
3	498 (1189)	1.9	1.9883; 2.0095; 2.2439
4	498 (5741), 1008 (14300)	2.5	1.9940; 2.0393; 2.2417

^a Molar extinction coefficients (M⁻¹) are given in parentheses.

^b Shoulder.

^c In solid state.

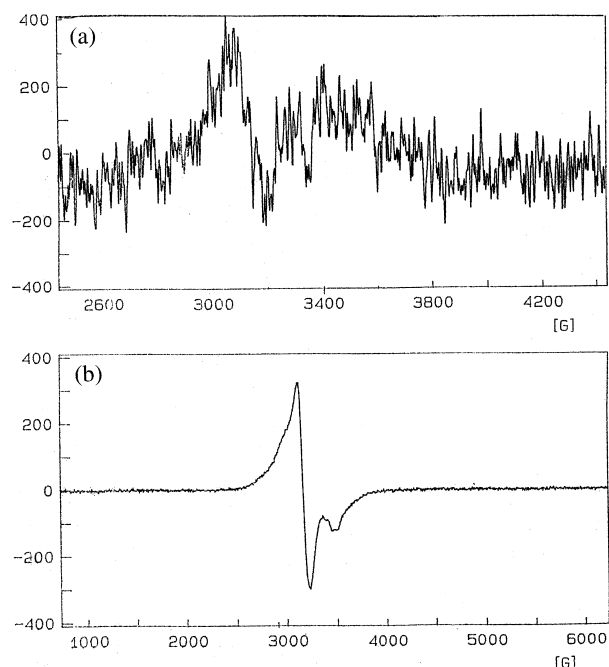


Fig. 2. ESR spectra of complex **1** in CH₂Cl₂ solution (a) and in solid state (b) at room temperature.

The ESR data discussed below are also in agreement with this argument. Values are shown in Table 2.

2.1.2. ESR spectra

The ESR spectra of mononuclear complexes **1** and **3** at room temperature in solid state exhibit one single signal,

characteristic of Cp(dppe)Fe^{III}X complexes [35–37]. Three well-separated features corresponding to the three components of the g tensor — expected for low symmetry pseudo-octahedral piano–stool complexes — were observed (see Fig. 2). Data are shown in Table 2. This indicates that the signal observed in both cases may correspond to the unpaired electron centred on the metal. The signal corresponding to the TCNE⁻ and TCNQ⁻ radical ligands was not observed, probably due to intramolecular spin coupling between the TCNX⁻ molecules in the solid state. Consistent with this, in CH₂Cl₂ solution the ESR spectra of **1** and **3** exhibit several complex signals with various features (see Fig. 2), which presumably include the signal of Cp(dppe)Fe^{III}L as well as the signals of TCNX⁻. As found for other LnM(η^1 -TCNX⁻) complexes [38,39], owing to the lowered symmetry, 16 (four different nitrogen) or 1296 (four different nitrogen and four different ¹H) lines for TCNE and TCNQ, respectively, could be observed.

2.1.3. Cyclic voltammetry

Mononuclear systems are reduced at more negative potentials than TCNX ligands (Table 3). This is a consequence of metal-to-ligand electron transfer in the ground state, which leaves either the single reduced ligand or the oxidized metal fragment available for reduction at relatively negative potentials.

Oxidation of the complexes is almost always irreversible; it may thus be safely assumed that these are metal-based. Thus peak potentials of about 0.7–0.8 V versus SCE

Table 3
Electrochemical data^a for TCNX ligands and their complexes

Compound	$E_{1/2}^{\text{ox}}$ (metal)	E_1^{red} (0/1-) ^d	E_2^{red} (-/2-) ^d
TCNE		0.18	-0.85
[Cp(dppe)Fe(TCNE)]PF ₆ (1)	0.83 ^b	-0.61	-0.95
[{Cp(dppe)Fe} ₂ (TCNE)](PF ₆) ₂ (2)	0.89, 0.70 ^c	-0.53	-0.88
TCNQ		0.25	-0.31
[Cp(dppe)Fe(TCNQ)]PF ₆ (3)	0.78 ^b	-0.49	-0.70
[{Cp(dppe)Fe} ₄ (TCNQ)](PF ₆) ₄ (4)	0.93, 0.75 ^c	-0.65	-0.80

^a In CH₂Cl₂-0.1 M Bu₄NPF₆; potential (in V) vs. SCE.

^b Anodic peak potential are given for irreversible oxidation processes.

^c Two very near quasi-reversible waves were observed.

^d Quasi-reversible waves.

(saturated calomel electrode) for complexes $[\text{Cp}(\text{dppe})\text{-Fe}(\text{nitrile})]\text{PF}_6$ have been observed [22–25].

2.1.4. Electronic spectroscopy

Complexes **1** and **3** exhibit intense bands at about 545 and 619 nm, which are typical of the absorption behaviour of $[\text{Cp}(\text{dppe})\text{Fe}^{\text{III}}\text{L}](\text{PF}_6)_2$ complexes [17–21] (Fig. 3). Table 2 summarizes the data obtained. No absorption was observed above 700 nm. This constitutes strong evidence for the $\text{Fe}^{\text{III}}\text{-(TCNX}^-)$ state because $\text{Fe}^{\text{II}}\text{-NCR}$ complexes exhibit only one band at about 450 nm [40].

2.2. Polynuclear complexes

TCNE or TCNQs react with an excess of $\text{Cp}(\text{dppe})\text{FeI}$ in the presence of NH_4PF_6 or TlPF_6 in CH_3OH or CH_2Cl_2 , respectively, to give black–green solids of composition $\{[\text{Cp}(\text{dppe})\text{Fe}]_2\text{TCNE}\}(\text{PF}_6)_2$ and $\{[\text{Cp}(\text{dppe})\text{Fe}]_4\text{-TCNQ}\}(\text{PF}_6)_4$. Similarly to complexes **1** and **3**, NMR studies are precluded due to the paramagnetism of the complexes. In agreement with this, the related complex $[\text{Ru}(\text{NH}_3)_4\text{-(}\mu\text{-TCNX)}]^{10+}$ is also paramagnetic [7]. No suitable crystals were obtained for X-ray structural determination of the complexes.

2.2.1. Infrared spectra

As pointed out by Kaim [8] and others [28], for $[\text{MLn}]_n\text{-(TCNX)}$ complexes some information about the structure of the complexes can be obtained from IR spectroscopy. The number and the pattern of bands observed by IR depend on the symmetry of the complexes; for the binuclear systems $[\text{MLn}]_2\text{-(}\mu\text{-TCNX)}$ three isomers can be expected: 1,2-*trans* (C_{2h}), 1,2-*cis* (C_{2v}) or 1,1' (C_{2v}). According to their symmetry, two or four bands could be observed for the isomers 1,2-*trans*, 1,1-*cis* or 1,2-*cis*, respectively. This is consistent with IR data for $[\text{MLn}]_n\text{-(}\mu\text{-TCNX)}$ complexes

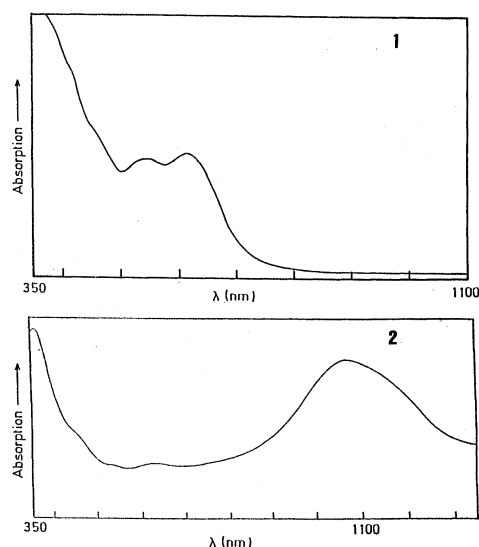


Fig. 3. Electronic absorption spectra of complexes **1** and **2** in CH_2Cl_2 solution.

having a 1,2-*trans* geometry: $[(\text{PPh}_3)_2(\text{CO})\text{Ir}]_2\text{TCNE}$ [29], (2176(m), 2097 vs); $[\text{L}'\text{L}_2\text{Cu}(\mu\text{-TCNE})\text{CuL}_2]_n$ [30], (2190, 2147); $[\text{Rh}_2(\text{O}_2\text{CCF}_3)_4]_2\text{TCNE}$ [31], (2230, 2210); $[\text{Tl}(\text{18-crown-6})\text{TCNQ}]$ [32], (2181, 2154); $[\text{Ru}(\text{PPh}_3)_2]_2\text{TCNQ}$ [33] (2170, 2140).

In agreement with this, the binuclear complex **2** exhibits two bands (one as a shoulder), suggesting the 1,2-*trans* configuration for this complex. This is the favoured configuration for bulky fragments [5] such as $\text{CpFe}(\text{dppe})$. As expected for tetranuclear complexes (with a slightly perturbed D_{2h} symmetry), two bands are observed for complex **4**. Thus complexes $[\text{Ru}(\text{NH}_3)_5\text{-(}\mu_4\text{-TCNX)}]$ and $[\text{C}_5\text{Me}_5\text{-Mn}(\text{CO})_2]_4\text{-(}\mu_4\text{-TCNX)}$ exhibit bands at: 2163, 2121 cm^{-1} for the Ru–TCNE complex; 2153, 2096 cm^{-1} for the Ru–TCNQ complex; 2160, 2110 cm^{-1} for the Mn–TCNE complex; and 2170, 2105 cm^{-1} for the Mn–TCNQ complex. As observed for similar $(\text{MLn})_2\text{TCNX}^{n+}$ and $(\text{MLn})_4\text{-TCNX}^{n+}$ complexes the highest intensity is displayed by the low-energy band, behaviour that is characteristic of polynuclear systems [6–10].

2.2.2. Magnetic measurements

The low magnetic moment for the binuclear complex **2** could be due to the delocalization of the unpaired electron between the two iron atoms, which couple antiferromagnetically with the unpaired electron of the TCNE^- ligand. On the other hand the tetranuclear complex **4** exhibits the highest magnetic moment, which could be due to the complex interaction of several paramagnetic Fe^{III} centres. Similar magnetic moments have been observed for tetranuclear $\{[\text{Cp}^*\text{Mn}(\text{CO})_2]_4\text{-(}\mu\text{-TCNE)}\}$ complexes [6–10].

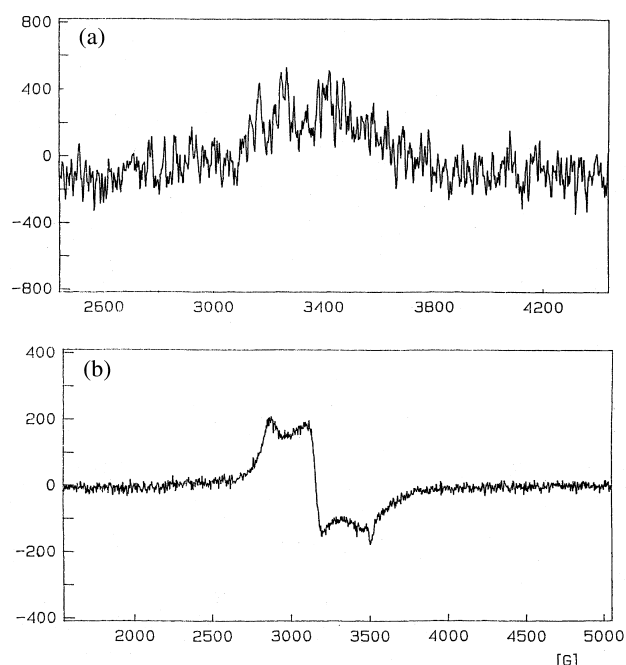


Fig. 4. ESR spectra of compound **2** in CH_2Cl_2 solution (a) and in solid state (b) at room temperature.

Table 4
Intervalence band parameters and derived electronic coupling parameter for the mixed-valence complexes ^a

Complex	ν_{\max} (cm ⁻¹)	ϵ (M ⁻¹ cm ⁻¹)	$\Delta\nu_{1/2}$ (cm ⁻¹)	α	d (Å)	V_{ab} (cm ⁻¹)	E_a (cm ⁻¹)	E_m (cm ⁻¹)	K_{th} (seg ⁻¹)
2	9320	968	1635	0.027	9.9	253	2330	9320	2.18×10^8
4	9978	5960	3159	0.063	14.2	625	2480	9921	1.22×10^8

^a In CH₂Cl₂ solution.

2.2.3. ESR spectra

The ESR spectrum of compound **2** in solid state shows a broad line exhibiting recognizable anisotropic features (Fig. 4), behaviour typical of delocalized mixed-valence systems [35–37]. The spectrum of compound **4** displays a similar pattern with the *g* factors summarized in Table 3. As observed for other multinuclear Ru–TCNX compounds [7], the ESR signal for the radical TCNX⁻ ligand was not observed. In CH₂Cl₂ solution, similarly to the mononuclear complexes, the signal of the iron centre as well as the complex signal of the organic TCNX⁻ radical were observed (see Fig. 4).

2.2.4. UV–Vis spectra

The UV–Vis spectra of complexes **2** and **4** revealed, in addition to absorptions typical for Cp(dppe)Fe^{III}L [17–21] and Cp(dppe)Fe^{II}L [40] chromophores, a new absorption band at about 1100 nm. The electronic spectrum of compound **2** in CH₂Cl₂ is shown in Fig. 3.

These observations coupled with data on similar Cp(dppe)Fe^{III}–L–Fe^{II}(dppe)Cp systems [11–21] allow us to assign this near-IR band to an intervalence transfer transition. Thus, on reducing the mixed valence complexes **2** and **4** with Red Al, sodium bis(2-methoxyethoxy)aluminium hydride, the intervalence absorption disappears.

2.2.5. Cyclic voltammetry

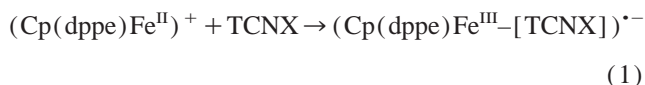
The reduction potential of the polynuclear complexes with TCNE and TCNQ (Table 3) are more negative than those of the corresponding free ligands; this is consistent with the electron transfer involved in the formation of the complexes, leaving the ligands as TCNX⁻ or TCNX²⁻.

Table 5
Electronic interaction parameter and electron transfer rate constants for **2**, **4** and other polynuclear mixed-valence complexes containing TCNE and TCNQ bridges

Complexes	V_{ab} (cm ⁻¹)	k_{et} (seg ⁻¹)
[{Cp [*] (CO) ₂ Mn} ₂ (μ-TCNE)] ^a	1302	1.27×10^{10}
[{(NH ₃) ₅ Ru] ₄ (μ-TCNE)](PF ₆) ₈ ^a	2980	2.7×10^8
[{(NH ₃) ₅ Ru] ₄ (μ-NCC(t-Bu)CN)] ^a	1256	1.26×10^9
[{(NH ₃) ₅ Ru] ₄ (μ-TCNQ)](PF ₆) ₈ ^a	1860	2.1×10^9
[{Cp(dppe)Fe} ₂ (μ-TCNE)](PF ₆) ₂ ^b	253	2.2×10^8
[{Cp(dppe)Fe} ₄ (μ-TCNQ)](PF ₆) ₄ ^b	625	6.2×10^8

^a Determined using Eq. (4) and literature data [11–16,27–33] for the intervalence transition.

^b This work.



In the oxidation region of the metal fragment, the cyclic voltammogram exhibits two non-well-defined waves which probably involve the oxidation of the metal centres. The difference in peak potential indicates a considerable coupling between the metal centres. From the wave separation, the comproportionation constant, K_c , relative to the following equilibrium:



can be computed as $K_c = 1626$ and 1202 for complexes **2** and **4**, respectively. The relatively high K_c values indicate a considerable electronic interaction between the iron atoms.

2.2.6. Electronic interaction in the mixed-valence species

Information about the degree of metal–metal interaction in the mixed-valence complexes can be obtained from the intervalence absorption band using the Hush formalism [11–16,41–45]. According to this, the degree of delocalization parameter is given by the formula:

$$\alpha = \frac{(4.2 \times 10^{-4}) \epsilon_{\max} \Delta\nu_{1/2}}{\nu_{\max} d^2} \quad (3)$$

where $\Delta\nu_{1/2}$ is the bandwidth at half-maximum (cm⁻¹), ϵ_{\max} is the maximum extinction coefficient, ν_{\max} is the band position (cm⁻¹) and d is the metal–metal distance in Å. Because no X-ray determination is available for complexes **2** and **4**, the metal–metal distance was estimated from structural data for similar complexes [46–48]. The α values shown in Table 4 indicate a class II Robin-Day system.

On the other hand the electronic coupling term, V_{ab} , can be determined by the following formula [41–45]:

$$V_{ab} = \alpha^{1/2} \nu_{\max} \quad (4)$$

The calculated values, displayed in Table 4, indicate a more or less strong metal–metal coupling, although somewhat less than for the cyanide ligand. From intervalence transfer transition data for other organometallic systems, the interaction parameter V_{ab} was estimated using Eq. (4). Values shown in Table 5 for other complexes indicate that metallic fragments such as (NH₃)₅Ru permit a stronger interaction than the iron fragment, which can be due to steric hindrance of the Cp(dppe)Fe⁺ arising from the bulky dppe [46]. From data

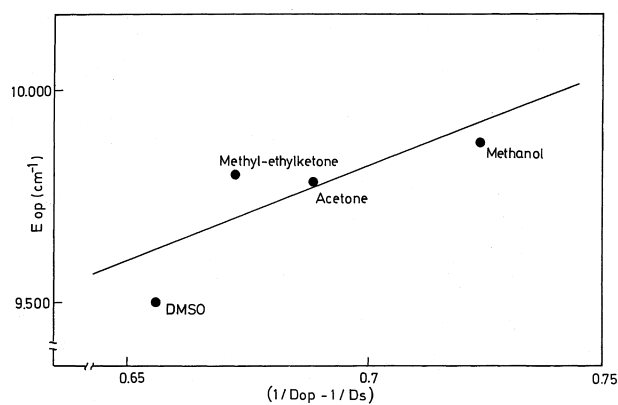


Fig. 5. Plot of intervalence absorption energy for E_{op} vs. $(1/D_{op} - 1/D_s)$.

in Table 5, it can also be concluded that the interaction between the metal centres is highly dependent on the nature of the organometallic fragment.

An approximate estimation of the rate of electron transfer between the metal centres in complexes **2** and **4** can be made using the expression [41–45]:

$$k_{th} = \left[\frac{2\pi(V_{ab})^2}{h} \right] \left[\frac{\pi}{KTE_m} \right]^{1/2} \left[e \left(-\frac{E_a}{RT} \right) \right] \quad (5)$$

where $E_m = E_{op}$ and $E_a = [(E_m)^2/4E_m]$. E_m , the total reorganization energy, has two components: the outer-reorganization energy E_o , and the inner-reorganization energy E_i ; thus $E_m = E_i + E_o$.

Although these equations differ in absolute values from those measured experimentally, comparison for a related series of compounds is valid [18]. The values about 10^8 s^{-1} calculated for compounds **2** and **4** indicate a fast electron transfer between the iron atoms. Similar rates are obtained using Eq. (5) for other organometallic systems, as can be seen in Table 5. The similar k_{et} values, notwithstanding the different organometallic fragment, mean that the nature of the bridge is most important in determining the electron transfer rate. It is interesting to compare the TCNX ligands as bridges with the cyanide bridging ligand for which electron-transfer rates of 10^4 s^{-1} were estimated in the mixed-valence complexes $[\text{Cp}(\text{dppe})\text{Fe}-\text{CN}-\text{MLn}]\text{PF}_6$ ($\text{MLn} = \text{Cp}(\text{dppe})\text{Fe}, \text{Mn}(\text{CO})_2(\text{dpmm})\text{P}(\text{OPh})_3$) [18].

Table 6
Solvent dependence of the intervalence transition in complexes **2** and **4**

Complex	Solvent	E_{op} (cm ⁻¹)	$(1/D_{op} - 1/D_s)$	E_i (cm ⁻¹)	E_o (cm ⁻¹)	E_m
2	Dimethylsulfoxide (DMSO)	9128	0.6551	6621	2587	9128
2	Acetone	9238	0.6886			
2	MeOH	9208	0.7234			
2	CH ₂ Cl ₂	9320	0.5899			
4	DMSO	9501	0.6550	8394	1448	9501
4	MeOH	9872	0.7234			
4	Ethyl methyl ketone	9799	0.6722			
4	Acetone	9780	0.6886			
4	CH ₂ Cl ₂	9978	0.5899			

The solvent effect on the intervalence transition gives information about the reorganization energy arising from rearrangements of the inner and outer coordination spheres [49,50]. With the assumption of a dielectric continuum model, the dependence of E_{op} on solvent polarization is given by:

$$E_{op} = E_i + E_o \quad (6)$$

$$E_{op} = E_i + e^2 \left(\frac{1}{2a_1} + \frac{1}{2a_2} - \frac{1}{d} \right) \times \left(\frac{1}{D_{op}} - \frac{1}{D_s} \right)$$

The intercept of a plot of E_{op} versus $(1/D_{op} - 1/D_s)$ for several solvents affords the E_i values (Fig. 5 and Table 6). From Eq. (6) the outer-sphere reorganizational parameters E_o can be estimated. Values for complexes **2** and **4** and for other complexes containing the $\text{CpFe}(\text{dppe})$ moiety are shown in Table 6. Some comments can be made from this data: comparing the E values for complexes **2** and **4**, mostly larger variations on the outer-reorganizational parameters than for the inner-reorganization values are observed (differences of 21% on E_i and of 43% on E_o are observed). This can be explained by the similar metal–ligand vibration modes involved in the electron-transfer process. Attention must be drawn to the high inner-reorganization energies involved in electron-transfer events in the complex $\{[\text{Cp}(\text{dppe})]_2-(\mu\text{-S}-\text{C}_5\text{H}_5\text{N})\}(\text{PF}_6)_2$. This may be due to an enhanced change on vibrational modes of the thiopyridine ligand upon electron transfer.

It is interesting to note that, although the complexes displayed in Table 7 all have the same fragment $\text{CpFe}(\text{dppe})$, the reorganization energy is very different. For instance, compare $E_m = 12\,697 \text{ cm}^{-1}$ for $[\text{CpFe}(\text{dppe})]_2-(\mu\text{-S}-\text{C}_5\text{H}_5\text{N})\}(\text{PF}_6)_2$ [21] with $E_m = 6038 \text{ cm}^{-1}$ for $\{[\text{CpFe}(\text{dppe})]_2-\mu\text{-CN}\}\text{PF}_6$ [18].

This means that, for this series, the reorganizational energy is highly dependent on some properties of the bridge ligand. Because the data in Table 7 indicate that the main contribution to the reorganizational energy arises from the inner-reorganization energy, the observed variations E_m might stem from changes in the vibrational mode of the bridging ligand.

Recent studies of electron transfer in the mixed-valence systems $[(\text{NC})_5\text{M}^{\text{II}}-\text{CN}-\text{Ru}^{\text{III}}(\text{NH}_3)_5]^-$ ($\text{M} = \text{Fe}$ or Ru)

Table 7

Solvent reorganization energies ^a for complexes **2**, **4** and other related complexes containing the moiety CpFe(dppe)⁺

Complex	E_i (cm ⁻¹)	E_o (cm ⁻¹)	E_m (cm ⁻¹)
[{CpFe(dppe)} ₂ -(μ-TCNE)](PF ₆) ₂	8394	1448	9842
[{CpFe(dppe)} ₄ -(μ-TCNQ)](PF ₆) ₄	6621	2587	9208
[{CpFe(dppe)} ₂ -(μ-S-C ₅ H ₄ N)](PF ₆) ₂	12470	227	12697
[{CpFe(dppe)} ₂ -(μ-CN)]PF ₆	2096	3942	6038

^a Values of E_m , E_i and E_o were determined from E_{op} vs. $(1/D_{op} - 1/D_s)$ plots. Values for complexes other than complexes **2** and **4** were taken from [11–21].

have shown that a large part of the reorganization energy comes from modes assigned to the bridging ligand [51,52].

Comparing the reorganizational values with electron-transfer rates it can be observed that there does not exist a correlation between them. According to semiclassical electron-transfer theory [41–45], electron-transfer reaction rates (k_{et}) are governed by three parameters (Eq. (5)): (1) the electronic coupling (V_{ab}) between reactants and products, (2) the free-energy change for the reaction (ΔG°) and (3) the total reorganization energy.

From Tables 5 and 7 it can be seen that no correlation exists between k_{et} and the electron coupling or the reorganization energy. However, the electron-transfer rate appears to be related to ΔG° through the relation $E_a = (E_{op})^2 / (E_{op} - \Delta G^\circ)$. In fact, a linear correlation between $\ln(k_{th})$ and E_a holds, as shown in Fig. 6. Furthermore, this expression has the shape of the most general and simple relationship between k_{et} and E_a , the classical Marcus equation $k_{et} = Ae^{-E_a}$ [41–45]. We believe that this is a remarkable example where the general electron rate theory of Marcus works well in mixed-valence complexes.

2.3. Nature of the electron transfer in binuclear complexes **2** and **4**

The efficient and fast electron transfer between the metal centres in complexes **2** and **4** can be explained by considering the molecular orbitals involved in the Fe–N interaction. These can be adequately established from an orbital interaction diagram built from the molecular orbital (MO) fragments of CpFe(dppe)⁺ and nitriles [53–56]. As shown in Fig. 7, the HOMO of complexes involves a π -delocalized molecular orbital throughout the Fe–TNCX–Fe moiety.

3. Experimental

All operations were conducted under a pure dinitrogen or argon atmosphere using standard Schlenk and glovebox techniques. Solvents were dried according to established protocols and degassed prior to use. Unless otherwise specified, reagents were obtained from commercial supplies and used as received. Magnetic measurements were carried out by Gouy's method at room temperature using a Johnson Matthey magnetic susceptibility balance with tetrathiocyanate cobaltate(II) as calibrant balance. ESR spectra were recorded on

Bruker ECS 106 spectrometer. FTIR spectra were recorded on an FT-IR Perkin Elmer 2000 spectrophotometer. Electronic absorption spectra were recorded on a Shimadzu UV 160. Cyclic voltammetry was performed on a three-electrode configuration (glassy-carbon working electrode, saturated calomel as reference) with 0.1 M solution of NH₄PF₆ as electrolyte support in CH₂Cl₂. Cp(dppe)FeI was prepared as previously reported [22–25].

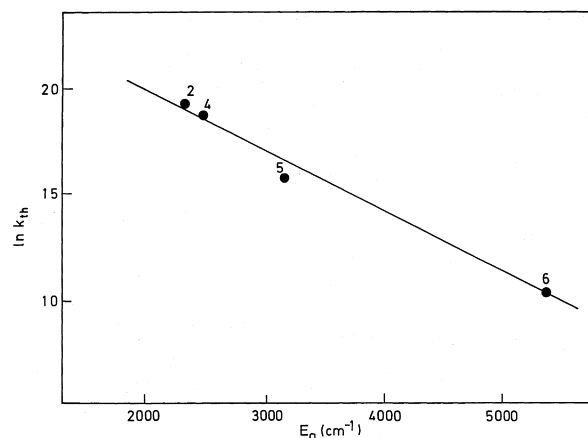


Fig. 6. Estimated electron-transfer rates vs. activation energy E_a for complexes **2**, **4**, [{CpFe(dppe)}₂-(μ-S-C₅H₄N)](PF₆)₂ (**5**) and [{CpFe(dppe)}₂-(μ-CN)]PF₆ (**6**).

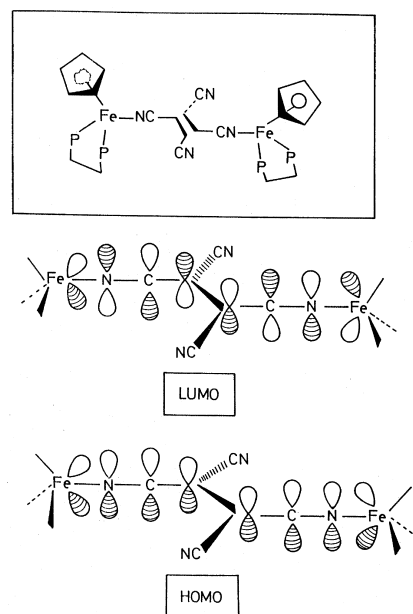


Fig. 7. Proposed HOMO-LUMO of complexes **2** and **4**.

3.1. $[Cp(dppe)Fe-(TCNE)]PF_6$ (**1**)

A solution of $Cp(dppe)FeI$ (70 mg, 0.10 mmol) in 20 ml of CH_3OH was added dropwise over 0.03 g, 0.23 mmol of $C_2(CN)_4$ and 0.03 g, 0.18 mmol of NH_4PF_6 . The mixture was stirred at room temperature for 24 h. The reaction mixture was then evaporated to dryness, and the solid residue redissolved in 30 ml and the solution filtered through Celite and evaporated to about 15 ml. After this a black solid was formed, which was decanted and washed twice with hexane–ether and dried in vacuo. Yield: 28 mg (29%). *Anal. Calc.* for $C_{41}H_{29}F_6N_4P_3Fe \cdot CH_2Cl_2$: C, 52.08; H, 3.54; N, 6.38. Found: C, 51.73; H, 4.02; N, 5.90%.

3.2. $\{[Cp(dppe)Fe]_2-(\mu-TCNE)\}(PF_6)_2$ (**2**)

To a solution of $Cp(dppe)FeI$, 0.15 g, 0.23 mmol in 10 ml of CH_3OH , was added dropwise slowly over 0.015 g, 0.11 mmol of $C_2(CN)_4$ in 20 ml of CH_3OH in the presence of NH_4PF_6 (0.03 g, 0.18 mmol). The mixture was stirred at room temperature for 24 h and then concentrated to dryness under reduced pressure. The solid was dissolved in CH_2Cl_2 (30 ml) and filtered through Celite. The solution was concentrated in vacuum to about 15 ml and the black solid precipitated was washed twice with hexane–ether and dried in vacuo. Yield: 0.045 g (28%). *Anal. Calc.* for $C_{72}H_{58}F_{12}N_8P_2Fe_2$: C, 62.26; H, 4.4; N, 5.0. Found: C, 61.7; H, 5.0; N, 5.0%.

3.3. $[Cp(dppe)Fe-(TCNQ)]PF_6$ (**3**)

A solution of $Cp(dppe)FeI$, 0.15 g, 0.23 mmol in 10 ml of CH_3OH , was added dropwise over 0.07 g, 0.34 mmol of TCNQ and in the presence of NH_4PF_6 (0.06 g, 0.36 mmol). Following the procedure outlined for separation and purification of compound **1**, 0.2 g of black solid was obtained. Yield: 68%. *Anal. Calc.* for $C_{43}H_{33}F_6N_4PFe \cdot CH_2Cl_2$: C, 55.43; H, 3.6; N, 5.8. Found: C, 54.3; H, 3.0; N, 4.8%.

3.4. $\{[Cp(dppe)Fe]_4-(\mu-TCNQ)\}(PF_6)_4$ (**4**)

To a solution of $Cp(dppe)FeI$, 0.15 g, 0.23 mmol in 20 ml of CH_3OH , was added dropwise slowly over 0.03 g, 0.14 mmol of TCNQ in 20 ml of CH_3OH in the presence of NH_4PF_6 (0.04 g, 0.25 mmol). The mixture was stirred at room temperature for 24 h. Separation and purification procedures similar to that for compound **3** afforded a black powder. Yield: 0.2 g (48%). *Anal. Calc.* for $C_{136}H_{120}F_{24}N_4P_4Fe_4 \cdot 2CH_2Cl_2$: C, 57.09; H, 4.2; N, 1.96. Found: C, 55.39; H, 4.26; N, 2.6%.

3.5. Preparation of complexes **1–4** using $TlPF_6$ as halide abstractor and CH_2Cl_2 as solvent

Similar compounds were obtained using the following typical procedure.

3.5.1. $[Cp(dppe)Fe-(TCNE)]PF_6$

A mixture of 0.15 g, 0.25 mmol of $Cp(dppe)FeI$, 0.04 g, 0.31 mmol of TCNE and 0.16 g, 0.45 mmol of $TlPF_6$ (**caution**: thallos salts are very poisonous and should be handled with care) in 30 ml of CH_2Cl_2 was stirred at room temperature for 3 days. The solution was then filtered through Celite and the filtrate was removed in vacuo to about 15 ml. The black solid precipitated was isolated by decantation and washed twice with n-hexane–ether, and dried in vacuo to give 0.12 g, 60% yield.

Acknowledgements

Financial support of this work from D.I.D., Universidad de Chile (Project 98-018), is gratefully acknowledged.

References

- [1] K.R. Dunbar, *Angew. Chem., Int. Ed. Engl.* 35 (1996) 1659.
- [2] J.S. Miller, A.J. Epstein, *Angew. Chem.* 106 (1994) 399.
- [3] J.S. Miller, A.J. Epstein, *Angew. Chem., Int. Ed. Engl.* 33 (1994) 385.
- [4] J.S. Miller, *Adv. Mater.* 6 (1994) 322.
- [5] W. Kaim, M. Moscherosch, *Coord. Chem. Rev.* 129 (1994) 157.
- [6] E. Waldhor, W. Kaim, M. Lawson, J. Jordanov, *Inorg. Chem.* 36 (1997) 3248.
- [7] M. Moscherosch, E. Waldhor, H. Binder, W. Kaim, J. Fiedler, *Inorg. Chem.* 34 (1995) 4326.
- [8] R. Gross-Lannert, W. Kaim, B. Olbrich-Deussner, *Inorg. Chem.* 29 (1990) 5046.
- [9] R. Gross-Lannert, W. Kaim, *Angew. Chem., Int. Ed. Engl.* 26 (1987) 251.
- [10] W. Kaim, T. Roth, B. Olbrich-Deussner, R. Gross-Lannert, J. Jordanov, E.K.H. Roth, *J. Am. Chem. Soc.* 114 (1992) 5693.
- [11] J. Fabian, K. Zahradnik, *Angew. Chem.* 101 (1989) 693.
- [12] J. Fabian, K. Zahradnik, *Angew. Chem., Int. Ed. Engl.* 28 (1989) 677.
- [13] D. Astruc, *Acc. Chem. Res.* 30 (1997) 383.
- [14] D. Astruc, *Electron Transfer and Radical Processes in Transition-Metal Chemistry*, VCH, New York, 1995.
- [15] D. Astruc, *Acc. Chem. Res.* 12 (1986) 377.
- [16] M.H. Desbois, D. Astruc, J. Guillin, F. Varret, A.X. Trautwein, G. Villaneuve, *J. Am. Chem. Soc.* 111 (1989) 5800.
- [17] G. Barrado, G.A. Carriedo, C. Díaz, V. Riera, *Inorg. Chem.* 30 (1991) 4416.
- [18] C. Díaz, A. Arancibia, *Inorg. Chim. Acta* 269 (1998) 246.
- [19] C. Díaz, C. Leal, N. Yutronic, *J. Organomet. Chem.* 516 (1996) 59.
- [20] C. Díaz, *Polyhedron* 16 (1997) 999.
- [21] C. Díaz, A. Arancibia, unpublished results.
- [22] C. Díaz, N. Yutronic, *Synth. React. Inorg. Met.-Org. Chem.* 27 (1997) 119.
- [23] C. Díaz, R. Latorre, *Bol. Soc. Chil. Quim.* 37 (1992) 211.
- [24] C. Díaz, A. Arancibia, *Bol. Soc. Chil. Quim.* 43 (1998) 303.
- [25] G.A. Carriedo, A. Arancibia, C. Díaz, N. Yutronic, E.P. Carreño, S.G. Granda, *J. Organomet. Chem.* 508 (1996) 23.
- [26] Strictly four bands must be observed for a C_s local symmetry of the η^1 -nitrogen linked ligand. However, three bands are normally observed, the fourth being observed as a shoulder, or masked for the most intense absorption; see [5–10] and references cited in [27].
- [27] B. Olbrich-Deubner, R. Gross, W. Kaim, *J. Organomet. Chem.* 366 (1989) 155.

- [28] J.L. Wesemann, M.H. Chisholm, *Inorg. Chem.* 36 (1997) 3258.
- [29] G.T. Yee, J.C. Calabrese, C. Vazquez, J.S. Miller, *Inorg. Chem.* 32 (1993) 377.
- [30] M.M. Olmstead, G. Speier, L. Szabó, *J. Chem. Soc., Chem. Commun.* (1994) 541.
- [31] F.A. Cotton, Y. Kim, *J. Am. Chem. Soc.* 221 (1993) 1.
- [32] M.C. Grossel, S.C. Wester, *J. Chem. Soc., Chem. Commun.* (1992) 1510.
- [33] I. Ito, S. Kitazume, A. Yamamoto, S. Ikeda, *J. Am. Chem. Soc.* 92 (1970) 3011.
- [34] M.M. Campos, C. Díaz, K. Figueroa, L. Padilla, N. Lara, G. Díaz, *Vibration Spectrosc.* 7 (1994) 61.
- [35] P. Hamon, I.R. Hamon, C. Lapinte, *J. Chem. Soc., Chem. Commun.* (1992) 1602.
- [36] P. Hamon, L. Toupet, J.R. Hamon, C. Lapinte, *J. Chem. Soc., Chem. Commun.* (1994) 931.
- [37] V. Mathias, S. Cron, L. Toupet, C. Lapinte, *Organometallics* 15 (1996) 5393.
- [38] T. Roth, W. Kaim, *Inorg. Chem.* 31 (1992) 1930.
- [39] S.E. Bell, J.S. Field, R.J. Haines, M. Moscherosh, W. Matheis, W. Kaim, *Inorg. Chem.* 31 (1992) 3269.
- [40] C. Díaz, B. Weiss, *Polyhedron* 12 (1993) 1403.
- [41] N.S. Hush, *Prog. Inorg. Chem.* 8 (1967) 391.
- [42] N.S. Hush, *Electrochim. Acta* 13 (1968) 1005.
- [43] N.S. Hush, *Coord. Chem. Rev.* 64 (1985) 135.
- [44] R.A. Marcus, N. Sutin, *Biochim. Biophys. Acta* 811 (1985) 265.
- [45] Y. Dong, J.T. Hupp, *Inorg. Chem.* 31 (1992) 3170.
- [46] P.E. Riley, C.E. Capshaw, R. Pettit, R.E. Davis, *Inorg. Chem.* 17 (1978) 408.
- [47] L. Ballester, M. Carmen Barral, A. Gutierrez, R. Jimenez-Aparicio, J. Martinez-Muyo, M.F. Perspiñan, M.A. Monge, C. Ruiz-Valero, *J. Chem. Soc., Chem. Commun.* (1991) 1395.
- [48] D. Ewan, A.J. Blake, T.A. Stephenson, M. Schroder, L.J. Tellouless, *J. Chem. Soc., Chem. Commun.* (1988) 1533.
- [49] M.D. Newton, N. Sutin, *Annu. Rev. Phys. Chem.* 35 (1984) 437.
- [50] N. Sutin, B.S. Brunschrig, C. Creutz, J.R. Winkler, *Pure Appl. Chem.* 60 (1998) 1817.
- [51] P. Forlano, F.D.C. Kiernik, O. Poizat, J. Olabe, *J. Chem. Soc., Dalton Trans.* (1997) 1595.
- [52] K.S. Door, P.O. Stoutland, R.B. Dyer, H.W. Woodruff, *Am. Chem. Soc.* 114 (1992) 3133.
- [53] For frontier OM of fragment Cp(dppe)Fe⁺ see: J.F. McGrady, T. Lowell, R. Stranger, M.G. Humphrey, *Organometallics* 16 (1997) 4004.
- [54] See also our studies in [40].
- [55] N.M. Kostic, R.F. Fenske, *Organometallics* 1 (1992) 1979.
- [56] For frontier OM for TCNX, see [6,8].